

# Pseudo-Cyclization through Intramolecular Hydrogen Bond Enables Discovery of Pyridine Substituted Pyrimidines as New Mer Kinase Inhibitors

Weihe Zhang,<sup>†,‡,§</sup> Dehui Zhang,<sup>†,‡,§</sup> Michael A. Stashko,<sup>†,‡</sup> Deborah DeRyckere,<sup>‡</sup> Debra Hunter,<sup>||</sup> Dmitri Kireev,<sup>†,‡</sup> Michael J. Miley,<sup>§</sup> Christopher Cummings,<sup>‡</sup> Minjung Lee,<sup>‡</sup> Jacqueline Norris-Drouin,<sup>†,‡</sup> Wendy M. Stewart,<sup>†,‡</sup> Susan Sather,<sup>‡</sup> Yingqiu Zhou,<sup>‡</sup> Gregory Kirkpatrick,<sup>‡</sup> Mischa Machius,<sup>§</sup> William P. Janzen,<sup>†,‡</sup> H. Shelton Earp,<sup>||,§</sup> Douglas K. Graham,<sup>‡</sup> Stephen V. Frye,<sup>†,‡,||</sup> and Xiaodong Wang<sup>\*,†,‡</sup>

<sup>†</sup>Center for Integrative Chemical Biology and Drug Discovery and <sup>‡</sup>Division of Chemical Biology and Medicinal Chemistry, Eshelman School of Pharmacy, University of North Carolina at Chapel Hill, Chapel Hill, North Carolina 27599, United States

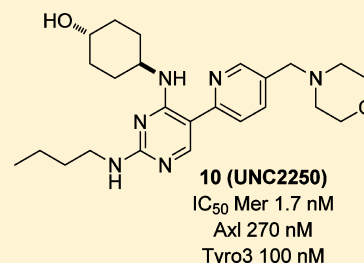
<sup>§</sup>Department of Pharmacology, School of Medicine, University of North Carolina at Chapel Hill, Chapel Hill, North Carolina 27599, United States

<sup>||</sup>Department of Medicine, UNC Lineberger Comprehensive Cancer Center, Chapel Hill, North Carolina 27599, United States

<sup>‡</sup>Department of Pediatrics, School of Medicine, University of Colorado Denver, Anschutz Medical Campus, Aurora, Colorado 80045, United States

## S Supporting Information

**ABSTRACT:** Abnormal activation or overexpression of Mer receptor tyrosine kinase has been implicated in survival signaling and chemoresistance in many human cancers. Consequently, Mer is a promising novel cancer therapeutic target. A structure-based drug design approach using a pseudo-ring replacement strategy was developed and validated to discover a new family of pyridinepyrimidine analogues as potent Mer inhibitors. Through SAR studies, **10** (UNC2250) was identified as the lead compound for further investigation based on high selectivity against other kinases and good pharmacokinetic properties. When applied to live cells, **10** inhibited steady-state phosphorylation of endogenous Mer with an IC<sub>50</sub> of 9.8 nM and blocked ligand-stimulated activation of a chimeric EGFR-Mer protein. Treatment with **10** also resulted in decreased colony-forming potential in rhabdoid and NSCLC tumor cells, thereby demonstrating functional antitumor activity. The results provide a rationale for further investigation of this compound for therapeutic application in patients with cancer.



## INTRODUCTION

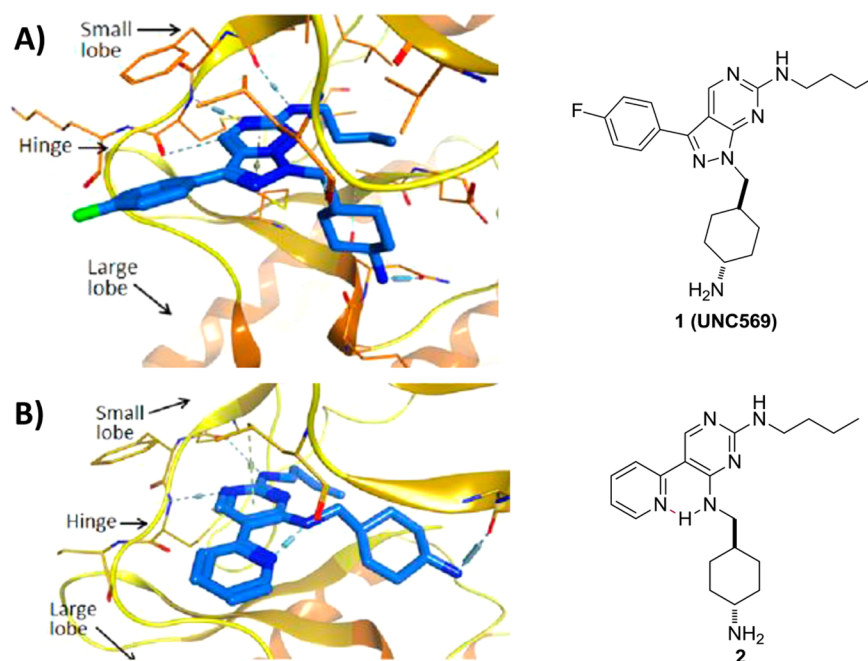
Mer belongs to the TAM (Tyro3, Axl, Mer) family of receptor tyrosine kinases (RTK) which share at least one common biological ligand: growth arrest-specific-6 (Gas6). Other ligands, including Protein S,<sup>1</sup> Tubbey,<sup>2</sup> TULP-1,<sup>2</sup> and Galectin-3,<sup>3</sup> can also stimulate Mer. Under normal physiologic conditions, Mer mediates the second phase of platelet aggregation, macrophage and epithelial cell clearance of apoptotic cells, modulation of macrophage cytokine synthesis, cell motility, and cell survival.<sup>4</sup> Abnormal activation or overexpression of Mer RTK has been implicated in neoplastic progression of many human cancers and has been correlated with poorer prognosis. For example, Mer is ectopically expressed in both B-cell and T-cell acute lymphoblastic leukemia (ALL), the most common pediatric malignancy, but is not expressed in normal mouse and human T- and B-lymphocytes at any stage of development.<sup>5</sup> Inhibition of Mer by si/sh-RNA knockdown sensitizes cells to chemotherapy-induced apoptosis and doubles survival in a xenograft model of acute leukemia.<sup>5c</sup> Similar effects are observed when Mer

expression is abrogated with shRNA in non-small-cell lung cancer (NSCLC) cells.<sup>6</sup> In addition, treatment of melanoma cells with a small molecule Mer inhibitor **UNC1062**<sup>7</sup> results in effects comparable to shRNA-mediated Mer inhibition, including reduced colony formation in soft agar and decreased invasion into collagen matrix.<sup>8</sup> Taken together, these data indicate that Mer is a novel therapeutic target for the treatment of ALL and other cancers that ectopically or overexpress Mer. Therefore, Mer inhibition with small molecule inhibitors may have clinical benefit either alone or in combination with chemotherapeutic agents.

We have previously developed several potent small molecule Mer inhibitors within the pyrazolopyrimidine scaffold.<sup>7,9</sup> However, we were motivated to explore other scaffolds to potentially increase selectivity within the TAM family of kinases<sup>9a</sup> and address solubility and pharmacokinetic properties required for further in vivo studies.<sup>7</sup> In order to design new

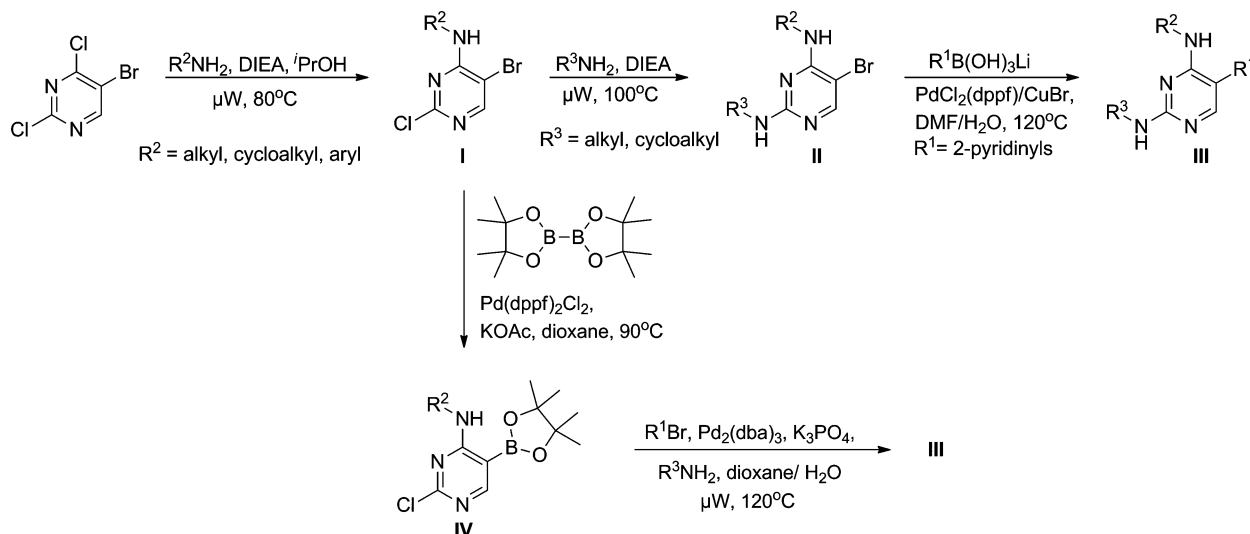
**Received:** September 9, 2013

**Published:** November 6, 2013



**Figure 1.** Structure-based design of a scaffold that relies on pseudo-ring formation through an intramolecular hydrogen bond: (A) X-ray structure of **1** in complex with Mer protein (kinase domain) (PDB code 3TCP); (B) docking model (based on X-ray structure PDB code 3TCP) of the designed molecule **2**.

### Scheme 1. General Synthetic Routes for Pyridinepyrimidine Analogues II



Mer inhibitors, we revisited the cocrystal structure of Mer in complex with **1** (UNC569) (Figure 1A).<sup>9a</sup> Wherein the inhibitor **1** is fully confined to the relatively small adenine pocket, including its flexible lipophilic butyl side chain, the pyrazole ring of **1** does not interact with any amino acid residue directly, suggesting that its main role might be to maintain the molecule's overall conformation. Replacing the pyrazole ring with a pseudo-ring<sup>10</sup> constrained by an intramolecular hydrogen bond as shown in compound **2** (Figure 1B) could potentially generate potent Mer inhibitors displaying different physicochemical properties when compared to pyrazolopyrimidines. Additionally, because the pseudo-ring in **2** is formed through a hydrogen bond between the pyridine nitrogen and the 4-amino group, it is less rigid than pyrazolopyrimidine and therefore is more likely to undergo “induced fit” to optimize its

interaction with the binding pocket. This scaffold would also simplify analogue synthesis and facilitate exploration of structure–activity relationships (SARs).

### CHEMISTRY

The proposed pyridinepyrimidines were synthesized using the route shown in Scheme 1. Starting with the commercially available compound 5-bromo-2,4-dichloropyrimidine, a  $S_NAr$  displacement of the chloride at the C4 position of the pyrimidine ring with an amine ( $R^2NH_2$ ) introduces substituents at the  $R^2$  position in **I**. The second  $S_NAr$  reaction at a higher temperature installs the  $R^3$  group at the C2 of the pyrimidine ring to yield the intermediate **II**. Finally, cross-coupling between **II** and a lithium trihydroxy borate salt of 2-pyridine or its derivatives provides the desired analogues **III**. We used 2-

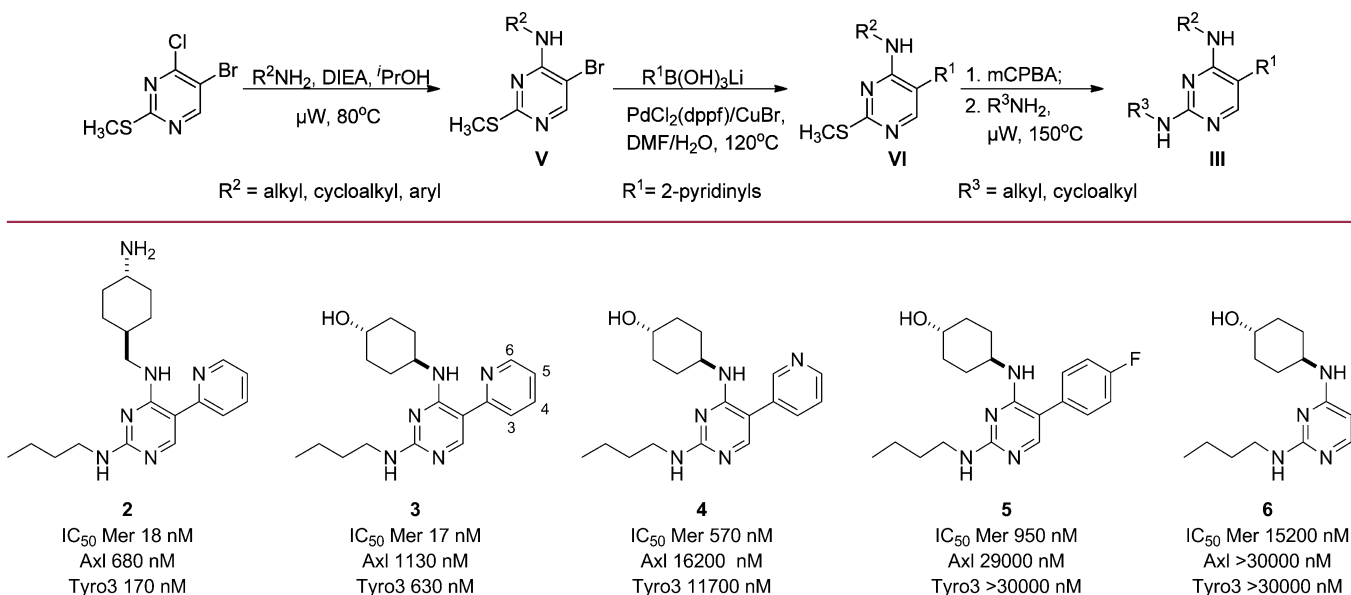
Scheme 2. General Synthetic Route To Explore SAR at the R<sup>3</sup> Position

Figure 2. Structures and enzymatic activities of compound 2 and its close analogues.

pyridyl trihydroxyborate salts for the coupling, as they are easily prepared.<sup>11</sup> In contrast, the corresponding boronic acid/ester of 2-pyridine and its derivatives are either very expensive or not readily available. Alternatively, **1** can also be converted to the corresponding boronic ester **IV** and subsequently be coupled with 2-chloropyridine or its derivatives to introduce the R<sup>1</sup> group at the C5 of the pyrimidine ring.<sup>12</sup> Overall, this route is optimal to explore the SAR at the R<sup>1</sup> site; it can also be used for SAR exploration at the R<sup>2</sup> and R<sup>3</sup> sites.

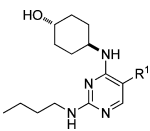
In addition, we developed an alternative route to synthesize analogues with different R<sup>3</sup> groups as shown in Scheme 2 because the most efficient way to prepare analogues was to place the exploration step at the last step of the synthesis. The S<sub>N</sub>Ar replacement of the chloride of commercially available 5-bromo-4-chloro-2-(methylthio)pyrimidine provides the intermediate **V** which can be transformed to **VI** via a Suzuki–Miyaura cross-coupling reaction with a lithium trihydroxyborate salt of 2-pyridinyl compounds. *m*-CPBA oxidation of **VI** followed by the second S<sub>N</sub>Ar replacement by various amines (R<sup>3</sup>NH<sub>2</sub>) yields the final products **III**.

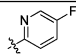
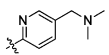
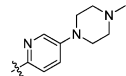
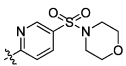
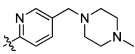
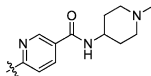
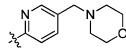
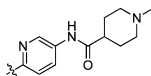
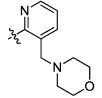
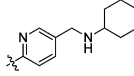
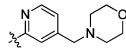
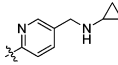
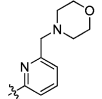
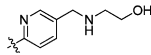
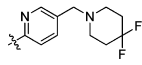
## RESULTS AND DISCUSSION

To validate the pseudo-ring strategy, we first synthesized compound **2** and its structurally close analogues (Figure 2) using the route shown in Scheme 1. Their activities against Mer kinase were then determined in a microfluidic capillary electrophoresis (MCE) assay.<sup>7,9a,13</sup> The IC<sub>50</sub> value of **2** was 18 nM, which was in the same range as that of the parent pyrazolopyrimidine compound **1**. Replacing the *trans*-4-aminocyclohexylmethylamino substitution in **2** with a *trans*-4-hydroxycyclohexylamino group also resulted in a potent Mer inhibitor **3**. This will likely diminish the undesired hERG activity present in **1** as previously demonstrated with **UNC1062**.<sup>7</sup> In contrast, the Mer activity decreased dramatically when the intramolecular hydrogen bond was disrupted either by moving the nitrogen of 2-pyridinyl to the C6 position of the pyridine ring (**4**, 34-fold) or by replacing it with a CH group (**5**, 56-fold). The complete removal of the 2-pyridinyl substitution

also rendered the corresponding **6** much less active (890-fold). Collectively, these results validate that the pseudo-ring design through an intramolecular hydrogen bond maintains a conformation similar to the pyrazolopyrimidine. Compared to **1**, compounds **2** and **3** are also more selective for Mer relative to Axl (38-fold and 67-fold, respectively) and Tyro3 (10-fold and 37-fold, respectively). This enhanced selectivity was fortuitous, but subsequent cocrystal structures (see below) may provide an explanation.

To develop potent Mer inhibitors with improved properties, we investigated the SAR with this newly discovered pyridinepyrimidine scaffold at the R<sup>1</sup>, R<sup>2</sup>, and R<sup>3</sup> positions. First, different substituents at the R<sup>1</sup> position were explored while fixing the R<sup>2</sup> site as a *trans*-4-hydroxycyclohexyl group and the R<sup>3</sup> site as a butyl group. As shown in Table 1, a fluorine at the 5-position of the pyridine ring did not affect the Mer activity of analogue **7** significantly while a larger group such as *N*-methylpiperazine at the same position led to a 6-fold more active analogue **8**. An extra methylene group between pyridine and *N*-methylpiperazine (**9**) was also tolerated. The *N*-methylpiperazine ring could be replaced by a morpholine ring to yield an equipotent analogue **10** (**UNC2250**). Interestingly, the substitution pattern on the pyridine ring played an important role in the activity of these compounds. The most active analogue **10** was generated from substitution at the 5-position of the pyridine ring, while a substituent at the 3-position (**11**) totally abolished the Mer activity, possibly because of steric clash of the substituents with the Mer protein backbone. The substitutions at the 4-position (**12**) and the 6-position of the pyridine ring (**13**) were tolerated but were not as active as when substituted at the 5-position (**10**). In addition, *N*-methylpiperazine at the 5-position of the pyridine in **9** could also be replaced with other groups such as 4,4-difluoropiperidine (**14**) and dimethylamine (**15**) without disrupting activity. Furthermore, other functionalities such as the sulfonamide (**16**), amide (**17**), or reversed amide (**18**) could be used to link the pyridine with another group such as morpholine (**16**) or *N*-methylpiperazine (**17** and **18**), resulting in similarly active analogues. However, the amide bond in **17** was not as stable to

Table 1. Preliminary SAR at the R<sup>1</sup> Position


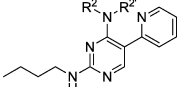
Compound	R <sup>1</sup>	IC <sub>50</sub> (nM) <sup>a</sup>			Compound	R <sup>1</sup>	IC <sub>50</sub> (nM) <sup>a</sup>		
		Mer	Axl	Tyro3			Mer	Axl	Tyro3
7		6.3	460	270	15		1.7	63	21
8		2.8	180	88	16		0.70	72	28
9		3.9	260	110	17		0.69	61	24
10		1.7	270	100	18		3.4	170	94
11		>30000	>30000	>30000	19		0.69	38	24
12		12	930	810	20		1.3	84	33
13		18		390	21		0.81	70	21
14		1.1	130	36					

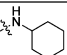
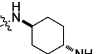
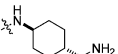
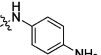
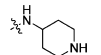
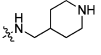
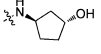
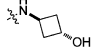
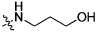

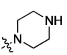
<sup>a</sup>Values are the mean of two or more independent assays.

hydrolysis as the reversed amide bond in **18**. 4-Amino-*N*-methylpiperidine was partially replaced by the solvent isopropanol during the workup of the amide bond coupling reaction (the reaction was quenched with a 1.0 N aqueous solution of NaOH or a saturated aqueous solution of NaHCO<sub>3</sub> and extracted with a mixture of isopropyl alcohol and CH<sub>2</sub>Cl<sub>2</sub> (1:10)). In addition, the secondary amines cyclohexylamino (**19**), cyclopropylamino (**20**), and even 2-hydroxyethylamino group (**21**) could serve as substituents on the methylene group at the 5-position of the pyridine ring. This is consistent with our docking model in which the R<sup>1</sup> group is exposed mostly to solvent, and there is space to accommodate a variety of groups. This feature makes this position ideal for substitutions that modify the physical and pharmacokinetic (PK) properties of these analogues. In general, this series is more potent for Mer than the other TAM kinases, and some are quite Mer-specific. For example, **10** is 160-fold more active for Mer versus Axl and 60-fold versus Tyro3.

Next, the SAR at the R<sup>2</sup> site was explored (Table 2). As predicted from the docking model, the polar group on the R<sup>2</sup> site is critical and can form a hydrogen bond with the carbonyl of Glu595. For example, removing the hydroxyl group from the

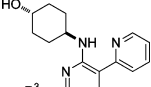
cyclohexyl substituent in compound **3** to produce analogue **22** dramatically decreased Mer activity (74-fold), while introducing an amino group at the same position of the cyclohexyl ring increased the activity of analogue **23**. Even an aminomethyl group at this position yielded a similarly active analogue **24**. However, introducing an aniline group at the R<sup>2</sup> position resulted in a 10-fold less inhibitory analogue (**25** versus **23**). A secondary amino group was less tolerated in analogues **26** and **27**. In addition, the cyclohexyl ring itself may have favorable hydrophobic interactions with the protein. When the ring size was reduced to a five- or four-membered ring, the activities of the corresponding analogues decreased (**28** and **29**) and the open-chained analogues **30** and **31** were further reduced in activity. In addition, the proton on the amino group which connects the substituents at the R<sup>2</sup> site to the pyrimidine ring played a key role in our design, as it forms an intramolecular hydrogen bond with the 2-pyridinyl maintaining the overall conformation of the molecule. Without this proton (**32**), the Mer activity was completely lost. Again, several of the analogues in Table 2 are quite Mer-selective (e.g., **23** has 300-fold selectivity for Mer over Axl and 50-fold over Tyro3).

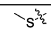
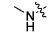
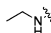
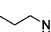
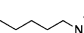
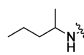
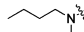
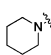
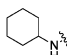
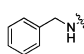
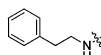
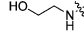
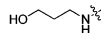
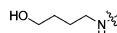
Table 2. SAR Study of R<sup>2</sup> Site


Compound	R <sup>2</sup> R <sup>2'</sup> N	IC <sub>50</sub> (nM) <sup>a</sup>		
		Mer	Axl	Tyro3
22		1250	>30000	>30000
23		1.8	550	84
24		4.5	180	58
25		18	830	280
26		34	1580	430
27		72	1280	390
28		160	3700	1370
29		200	2790	1340
30		1130	9890	4910
31		600	20800	4060
32		>30000	>30000	>30000

<sup>a</sup>Values are the mean of two or more independent assays.

Analogues were also synthesized to investigate the SAR at the R<sup>3</sup> position using the synthetic route shown in Scheme 2 (Table 3). On the basis of the X-ray crystal structure of **1** in complex with the Mer protein (Figure 1A), the NH from the butylamino side chain forms a hydrogen bond with the hinge region of the Mer protein. When a sulfur atom was placed at this position, the corresponding analogue **33** was much less active than analogue **34**. This was due to absence of this key hydrogen bond. Analogue **34** was a less potent Mer inhibitor compared to **3** because of the diminished hydrophobic interaction at the R<sup>3</sup> site. When the alkyl side chain at the R<sup>3</sup> position was made longer, the resulting analogues **35** and **36** gained activity until the side chain reached five carbons in length (**37**). Analogue **37** was equally potent to **3**. A branched methyl group at the  $\alpha$ -position of the NH (**38**) decreased the activity slightly. However, the activity dropped dramatically (22-fold) when the hydrogen on the NH was replaced with a

Table 3. Further SAR Study of R<sup>3</sup>


Compound	R <sup>3</sup> R <sup>3'</sup> N	IC <sub>50</sub> (nM) <sup>a</sup>		
		Mer	Axl	Tyro3
33		2700	>30000	>30000
34		540	3920	6850
35		170	3530	2580
36		50	6180	1590
37		19	650	440
38 <sup>b</sup>		44	8040	370
39		380	>30000	>30000
40		16500	>30000	>30000
41		83	20300	1160
42		110	>30000	300
43		14	430	80
44		320	18500	8940
45		220	15000	6140
46		44	3460	2930

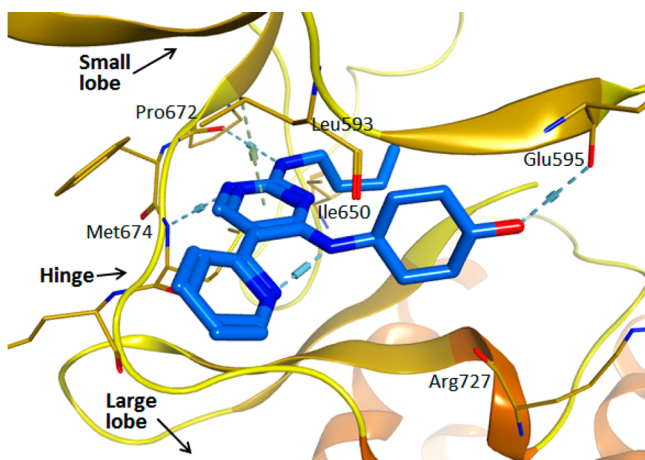
<sup>a</sup>Values are the mean of two or more independent assays. <sup>b</sup>Racemate.

methyl group (**39**), which further confirmed the importance of the hydrogen bond formed between the NH and the hinge region of the Mer kinase domain. This effect was more evident when a larger piperidine group was placed at the R<sup>3</sup> position; the corresponding analogue **40** lost almost all activity against Mer. A cycloalkyl group at this position had a similar effect as a branched alkyl side chain; analogue **41** had similar potency to **38**. A phenyl ring was also tolerated at the side chain, comparing analogues **42** to **35** and **43** to **36**. In addition, a polar hydroxyl group at the end of the alkyl side chain decreased the activity of the resulting analogues because of a weaker binding caused by a less favorable hydrophobic



contribution (44 vs 36, 45 vs 3). When the length of the side alkyl chain reached four carbons, the corresponding analogue 46 regained its activity comparable to 37, probably because of the vicinity of the polar hydroxyl group to the solvent front. Again, these analogues were quite Mer-selective compared to the pyrazolopyrimidines.

To provide a deeper insight into the binding interactions of the pyridine–pyrimidine inhibitors and afford structural guidance for further chemical optimization, a cocrystal structure of Mer in complex with compound 3 was obtained (Figure 3).



**Figure 3.** X-ray structure of 3 in complex with Mer kinase domain (PDB code 4M3Q).

In this structure, the inhibitor 3 demonstrates a binding mode in which the pyrimidine-2-amine group mimics the interactions of the cofactor's adenine with the backbone atoms of the hinge

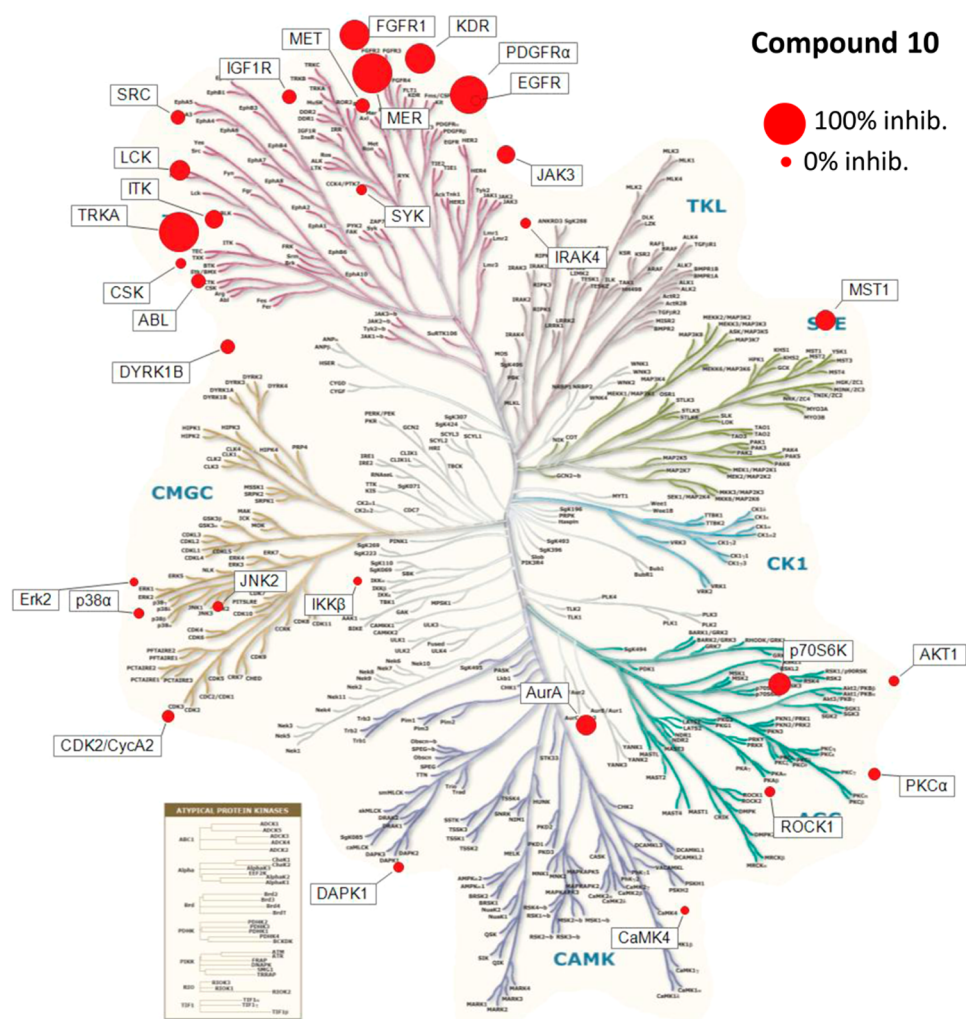
(residues Pro672 and Met674). Similar to the previously published structure of the Mer/1 complex, the aminobutyl R<sup>3</sup> substituent is bent within the adenine subpocket. Unlike the former structure, the hydroxyl group of the R<sup>2</sup> substituent forms a hydrogen bond with the backbone carbonyl of Glu595 (the analogous R<sup>2</sup> amino group of 1 interacts with Arg727). This difference is most likely because the cyclohexyl group was reoriented because of the intramolecular H-bond between the pyridine and 4-amino groups. It is noteworthy that one of the gate-forming residues, Ile650, is not conserved in the other two TAM family members. Axl and Tyro3 feature methionine and alanine, respectively, at this position. This variability is one likely reason for significant intrafamily selectivity. Consistent with the SAR outlined above, the R<sup>1</sup> substituent interacts mostly with the solvent and does not significantly impact the activity. Consequently, it can be utilized for tuning solubility and PK properties. Nevertheless, the freedom to modify R<sup>1</sup> has its limits, as demonstrated by compound 11, whose bulky pyridine–morpholine R<sup>1</sup> substituent precludes an efficient interaction with the hinge.

Four potent analogues (10, 14, 16, and 20) with distinctively different R<sup>1</sup> groups were chosen for PK studies (Table 4). The in vivo PK properties of these compounds were assessed in mice following intravenous (iv) or oral (po) administration (Table 4). All four compounds had high systemic clearance (69–149% of normal liver blood flow in mice). Among them 20 had the longest half-life (4.71 h) but also had an extremely high volume of distribution (56-fold higher than the normal volume of total body water in mice) and low plasma concentrations. Compound 14 had the best oral bioavailability (55%) but a high volume of distribution (20-fold), while 16 had a short half-life and low oral exposure. Compound 10 had a moderate half-life, clearance, and volume of distribution as well

**Table 4.** PK Profiles of 10, 14, 16, and 20

Compound	Structure	Route <sup>a</sup>	T <sub>1/2</sub> (h)	T <sub>max</sub> (h)	C <sub>max</sub> (ng/mL)	AUC <sub>last</sub> (h*ng/mL)	CL <sub>obs</sub> (mL/min/kg)	V <sub>ss</sub> (L/kg)	%F
10		IV	1.59	-	1975	794	62.2	3.90	-
		PO	-	0.25	162	180	-	-	23
14		IV	2.97	-	737	381	123	13.72	-
		PO	-	0.25	71	210	-	-	55
16		IV	0.91	-	1980	355	134	2.90	-
		PO	-	0.25	13.9	4.68	-	-	1.3
20		IV	4.71	-	277	376	130	39.02	-
		PO	-	0.50	33	103	-	-	27

<sup>a</sup>A dose of 3 mg/kg for both routes.



**Figure 4.** Kinase tree.

as reasonable oral bioavailability and good solubility and was thus chosen for characterization of kinase selectivity and further evaluation in cell-based studies of Mer activity.

The inhibitory activity of **10** against 30 kinases (detailed in Supporting Information) was determined at a concentration 100-fold above its Mer  $IC_{50}$  (Figure 4). The kinase panel selected emphasized tyrosine kinases along with a selection of serine/threonine kinases, providing a broad survey of kinase families. Five out of 30 kinases were inhibited greater than 50% in the presence of 180 nM **10**, and none of the serine/threonine kinases were appreciably inhibited.

In cell-based assays, **10** mediated inhibition of Mer phosphorylation in 697 B-ALL cells with an  $IC_{50}$  value of 9.8 nM (Figure 5). Mer phosphorylation was also inhibited in Colo699 NSCLC cells (Figure 6A). In addition to these effects on steady-state levels of Mer tyrosine phosphorylation, **10** efficiently inhibited ligand-dependent phosphorylation of a chimeric protein consisting of the extracellular and transmembrane domains of the epidermal growth factor (EGF) receptor and the intracellular tyrosine kinase domain of Mer (Figure 6B). Moreover, **10** incubation inhibited colony formation in soft agar cultures of the BT-12 rhabdoid tumor and the Colo699 NSCLC cell lines (Figure 7). In the Colo699 NSCLC cell line, the concentrations of **10** required to inhibit colony formation and Mer phosphorylation were similar. These

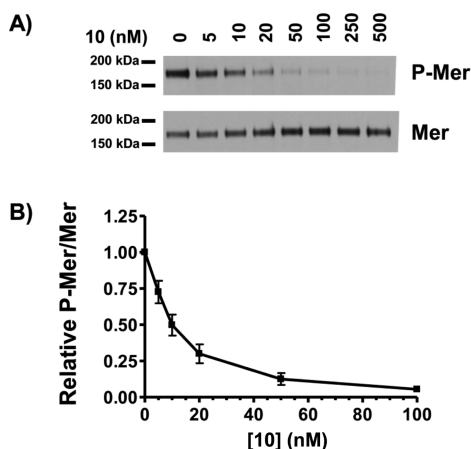
data suggest that the functional antiproliferative activity mediated by **10** resulted from Mer inhibition rather than a consequence of off-target inhibition of other kinases.

## CONCLUSIONS

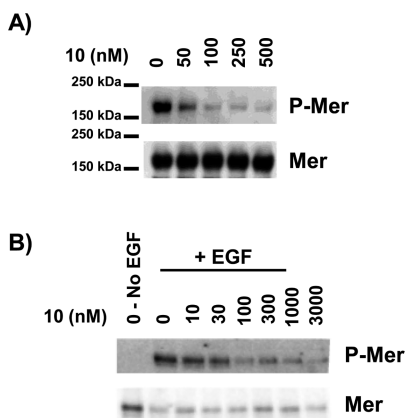
A new pyridinepyrimidine scaffold has been discovered and developed to create potent Mer kinase inhibitors by applying a structure-based drug design approach using a pseudo-ring replacement strategy. A cocrystal structure of Mer with one inhibitor (**3**) has been obtained and supports the predicted binding mode where an intramolecular hydrogen bond is used to induce conformational rigidity. The selectivity and PK properties of the lead compound **10** are promising, and further optimization of this series is ongoing. When applied to live cells, **10** efficiently inhibited both steady state and ligand-stimulated phosphorylation of Mer. Furthermore, treatment with **10** was sufficient to reduce colony-forming potential in both rhabdoid tumor cells and NSCLC cells, confirming functional antitumor activity mediated by **10** and suggesting the tractability of this new series to deliver clinically useful agents.

## EXPERIMENTAL SECTION

Details on the synthesis of all compounds are given in the Supporting Information. The purity of all tested compounds was determined by LC/MS to be >95%.

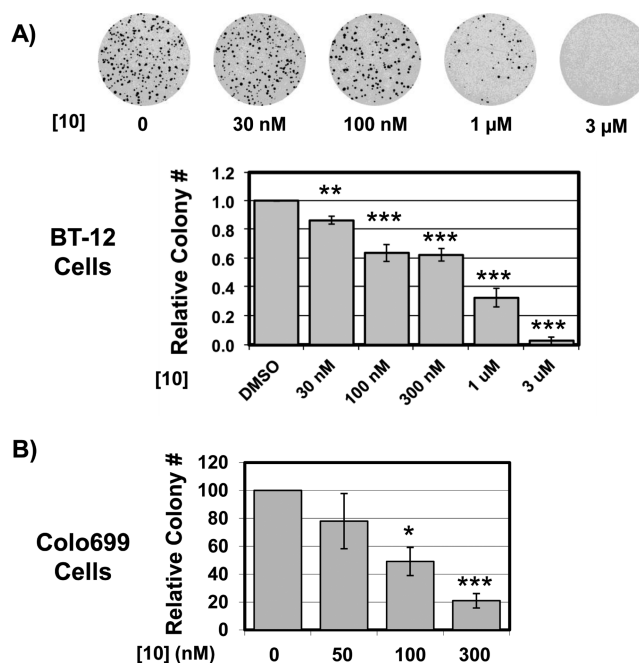


**Figure 5.** 10 inhibits Mer tyrosine kinase activation in acute leukemia cells. 697 B-ALL cells were treated with the indicated concentrations of 10 for 1 h. Pervanadate was added to cultures for 3 min to stabilize the phosphorylated form of Mer. Mer was immunoprecipitated from cell lysates, and total Mer protein and Mer phosphoprotein were detected by immunoblot. (A) Representative Western blots. (B) Relative levels of phospho-Mer and Mer proteins were determined. Mean values  $\pm$  standard error derived from three independent experiments are shown.  $IC_{50} = 9.8$  nM with a 95% confidence interval of 7.9–12.3 nM.



**Figure 6.** 10 inhibits Mer activation in adherent tumor cell lines. (A) Colo699 NSCLC cells were treated with 10 or vehicle for 72 h followed by treatment with pervanadate for 3 min. Whole cell lysates were prepared. Mer protein was immunoprecipitated, and phosphorylated and total Mer proteins were detected by Western blot. (B) 32D cells stably expressing a chimeric receptor consisting of the extracellular ligand-binding and transmembrane domains of the EGF receptor and the intracellular kinase domain of Mer were treated with 10 or vehicle for 1 h prior to stimulation for 15 min with 100 ng/mL EGF. Mer was immunoprecipitated from whole cell lysates and phosphotyrosine containing and total Mer proteins were detected by Western blot. Results shown are representative of four (A) or three (B) independent experiments.

**Microfluidic Capillary Electrophoresis (MCE) Assay.<sup>9a</sup>** Activity assays were performed in a 384-well, polypropylene microplate in a final volume of 50  $\mu$ L of 50 mM Hepes, pH 7.4, containing 10 mM  $MgCl_2$ , 1.0 mM DTT, 0.01% Triton X-100, 0.1% bovine serum albumin (BSA), containing 1.0  $\mu$ M fluorescent substrate (Table 5) and ATP at the  $K_m$  for each enzyme (Table 5). All reactions were terminated by addition of 20  $\mu$ L of 70 mM EDTA. After an 180 min incubation, phosphorylated and unphosphorylated substrate peptides (Table 5) were separated in buffer supplemented with 1 $\times$  CR-8 on a



**Figure 7.** 10 inhibits colony formation in solid tumor cell lines. (A) BT-12 rhabdoid tumor cells were cultured in soft agar containing 10 nM to 3  $\mu$ M 10 or vehicle only and overlaid with medium containing 10 or vehicle only. Medium and 10 were refreshed twice weekly. Colonies were stained and counted. Representative plates are shown. (B) Colo699 NSCLC cells were cultured in 0.35% soft agar overlaid with medium containing 10 or vehicle. Medium and 10 were refreshed 3 times per week. Colonies were stained and counted. Mean values  $\pm$  SEM derived from four independent experiments are shown. Statistically significant differences were determined using the Student's paired  $t$  test ((\*)  $p < 0.02$ , (\*\*)  $p < 0.01$ , (\*\*\*)  $P < 0.001$  relative to vehicle only).

**Table 5.** Assay Conditions for MCE Assays

kinase	peptide substrate	kinase (nM)	ATP ( $\mu$ M)
Mer	5-FAM-EFPIYDFLPAKKK-CONH <sub>2</sub>	2.0	5.0
Axl	5-FAM-KKKKEEYFFF-CONH <sub>2</sub>	120	65
Tyro	5-FAM-EFPIYDFLPAKKK-CONH <sub>2</sub>	10	21

LabChip EZ Reader equipped with a 12-sipper chip. Data were analyzed using EZ Reader software.

**Cell Based Assays for Mer Kinase Inhibition.** 697 B-ALL, 32D cells expressing a chimeric EGFR-MerTK receptor, BT-12 rhabdoid tumor, or Colo699 NSCLC cells were cultured in the presence of 10 or vehicle only for 1.0 h (697 B-ALL, 32D, BT-12 rhabdoid tumor) or 72 h (Colo699 NSCLC). Pervanadate solution was prepared fresh by combining 20 mM sodium orthovanadate in 0.9 $\times$  PBS in a 1:1 ratio with 0.3% (w/w) hydrogen peroxide in PBS for 15–20 min at room temperature. Cultures were treated with 120  $\mu$ M pervanadate prior to collection for preparation of whole cell lysates, immunoprecipitation of Mer, and analysis by Western blot.

697 B-ALL and Colo699 NSCLC cells were treated with pervanadate for 3.0 and 1.0 min, respectively. Cell lysates were prepared in 50 mM HEPES, pH 7.5, 150 mM NaCl, 10 mM EDTA, 10% glycerol, and 1% Triton X-100, supplemented with protease inhibitors (Roche Molecular Biochemicals, no. 11836153001). Mer protein was immunoprecipitated with a monoclonal anti-Mer antibody (R&D Systems, no. MAB8912) and protein G agarose beads (Invitrogen). Phospho-Mer was detected by Western blot using a polyclonal anti-phospho-Mer antibody raised against a peptide derived from the triphosphorylated activation loop of Mer. Nitrocellulose membranes were stripped, and total Mer protein was detected using a



second anti-Mer antibody (Epitomics Inc., no. 1633-1). For 697 B-ALL cells, relatively phosphorylated and total Mer protein levels were determined by densitometry using Image J software, and IC<sub>50</sub> values were calculated by nonlinear regression.

Confluent BT-12 rhabdoid tumor cultures were treated with pervanadate for 15 min. Confluent 32D cells expressing EGFR-MerTK chimeric protein were treated with 100 ng/mL EGF ligand for 15 min and were collected without pervanadate treatment. Cell lysates were prepared in 20 mM HEPES, pH 7.5, 50 mM sodium fluoride, 500 mM NaCl, 5.0 mM EDTA, 10% glycerol, and 1% Triton X-100, supplemented with protease inhibitors (10 µg/mL leupeptin, 10 µg/mL phenylmethylsulfonyl fluoride, and 20 µg/mL aprotinin) and phosphatase inhibitors (50 mM sodium fluoride and 1.0 mM sodium orthovanadate), and Mer protein was immunoprecipitated using a polyclonal rabbit anti-Mer antisera raised against a peptide derived from the C-terminal 100 amino acids of human Mer expressed as AST protein and protein A agarose beads (Santa Cruz Biotechnology). Phosphotyrosine-containing proteins were detected by Western blot with a monoclonal HRP-conjugated anti-phosphotyrosine antibody (Santa Cruz Biotechnology, no. sc-508). Antibodies were stripped from membranes, and total Mer levels were determined using a custom polyclonal rabbit anti-Mer antibody raised against a peptide derived from the catalytic domain of Mer.

32D-EMC suspension cultures were treated with the indicated of 10 or vehicle before stimulation with 100 ng/mL EGF (BD Biosciences no. 354010) for 15 min. Cells were centrifuged at 1000g for 5 min and washed with 1× PBS. Cell lysates were prepared in 20 mM HEPES (pH 7.5), 50 mM NaF, 500 mM NaCl, 5.0 mM EDTA, 10% glycerol, and 1% Triton X-100, supplemented with protease inhibitors (10 µg/mL leupeptin, 10 µg/mL phenylmethylsulfonyl fluoride, and 20 µg/mL aprotinin) and phosphatase inhibitors (50 mM NaF and 1.0 mM sodium orthovanadate), and Mer protein was immunoprecipitated using the polyclonal rabbit anti-Mer C-terminus antisera and protein A agarose beads (Santa Cruz Biotechnology). Phosphotyrosine-containing proteins were detected by Western blot with a monoclonal HRP-conjugated anti-phosphotyrosine antibody (Santa Cruz Biotechnology, no. sc-508). Antibodies were stripped from membranes, and total Mer levels were determined using the custom polyclonal rabbit anti-Mer antibody raised against a peptide derived from the catalytic domain of Mer.

**Soft Agar Colony Formation Assays.** BT-12 rhabdoid tumor cells (10 000 cells) were cultured in 2.0 mL of 0.35% soft agar containing 0.5× RPMI medium, 7.5% FBS, and the indicated concentrations of 10 or DMSO vehicle only and overlaid with 0.5 mL of 1× RPMI medium containing 15% FBS and 10 or DMSO vehicle only. Medium and 10 or vehicle were refreshed 2 times per week. Colonies were stained with thiazolyl blue tetrazolium bromide (Sigma Aldrich, no. M5655) and counted after 3 weeks.

Colo699 NSCLC cells (15 000 cells) were cultured in 1.5 mL of 0.35% soft agar containing 1× RPMI medium and 10% FBS and overlaid with 2.0 mL of 1× RPMI medium containing 10% FBS and the indicated concentrations of 10 or DMSO vehicle only. Medium and 10 or vehicle were refreshed 3 times per week. Colonies were stained with nitroretetrazolium blue chloride (Sigma Aldrich, no. N6876) and counted after 2 weeks.

## ■ ASSOCIATED CONTENT

### ● Supporting Information

Experimental details, characterization of all compounds, and selectivity profiling. This material is available free of charge via the Internet at <http://pubs.acs.org>.

### Accession Codes

The atomic coordinates for the X-ray crystal structure of 3 have been deposited with the RCSB Protein Data Bank under the accession code 4M3Q.

## ■ AUTHOR INFORMATION

### Corresponding Author

\*Phone: 919-843-8456. E-mail: [xiaodonw@unc.edu](mailto:xiaodonw@unc.edu).

### Author Contributions

#W.Z. and D.Z. contributed equally.

### Notes

The authors declare the following competing financial interest(s): D.D., D.K., W.P.J., H.S.E., D.K.G., S.V.F, and X.W. hold equity in Meryx, Inc.

## ■ ACKNOWLEDGMENTS

We thank Dr. Andrew McIver for his help on manuscript writing. This work was supported by the University Cancer Research Fund and Federal Funds from the National Cancer Institute, National Institutes of Health, under Contract No. HHSN261200800001E. The content of this publication does not necessarily reflect the views or policies of the Department of Health and Human Services, nor does mention of trade names, commercial products, or organizations imply endorsement by the U.S. Government.

## ■ REFERENCES

- (1) Chen, J.; Carey, K.; Godowski, P. J. Identification of Gas6 as a ligand for Mer, a neural cell adhesion molecule related receptor tyrosine kinase implicated in cellular transformation. *Oncogene* **1997**, *14* (17), 2033–2039.
- (2) Caberoy, N. B.; Zhou, Y.; Li, W. Tubby and Tubby-like protein 1 are new MerTK ligands for phagocytosis. *EMBO J.* **2010**, *29* (23), 3898–3910.
- (3) Caberoy, N. B.; Alvarado, G.; Bigcas, J.-L.; Li, W. Galectin-3 is a new MerTK-specific eat-me signal. *J. Cell. Physiol.* **2012**, *227* (2), 401–407.
- (4) (a) Linger, R. M. A.; Keating, A. K.; Earp, H. S.; Graham, D. K. TAM Receptor Tyrosine Kinases: Biologic Functions, Signaling, and Potential Therapeutic Targeting in Human Cancer. In *Advances in Cancer Research*; Academic Press: New York, 2008; Vol. 100, pp 35–83. (b) Linger, R. M. A.; Keating, A. K.; Earp, H. S.; Graham, D. K. Taking aim at Mer and Axl receptor tyrosine kinases as novel therapeutic targets in solid tumors. *Expert Opin. Ther. Targets* **2010**, *14* (10), 1073–1090. (c) Brandao, L.; Migdall-Wilson, J.; Eisenman, K.; Graham, D. K. TAM receptors in leukemia: expression, signaling, and therapeutic implications. *Crit. Rev. Oncogene* **2011**, *16* (1–2), 47–63.
- (5) (a) Graham, D. K.; Salzberg, D. B.; Kurtzberg, J.; Sather, S.; Matsushima, G. K.; Keating, A. K.; Liang, X.; Lovell, M. A.; Williams, S. A.; Dawson, T. L.; Schell, M. J.; Anwar, A. A.; Snodgrass, H. R.; Earp, H. S. Ectopic expression of the proto-oncogene Mer in pediatric T-cell acute lymphoblastic leukemia. *Clin. Cancer Res.* **2006**, *12* (9), 2662–2669. (b) Yeoh, E. J.; Ross, M. E.; Shurtleff, S. A.; Williams, W. K.; Patel, D.; Mahfouz, R.; Behm, F. G.; Raimondi, S. C.; Relling, M. V.; Patel, A.; Cheng, C.; Campana, D.; Wilkins, D.; Zhou, X.; Li, J.; Liu, H.; Pui, C. H.; Evans, W. E.; Naeve, C.; Wong, L.; Downing, J. R. Classification, subtype discovery, and prediction of outcome in pediatric acute lymphoblastic leukemia by gene expression profiling. *Cancer Cell* **2002**, *1* (2), 133–143. (c) Linger, R. M.; Lee-Sherick, A. B.; Deryckere, D.; Cohen, R. A.; Jacobsen, K. M.; McGranahan, A.; Brandão, L.; Wines, A.; Sawczyn, K. K.; Liang, X.; Keating, A. K.; Tan, A. C.; Earp, H. S.; Graham, D. K. Mer receptor tyrosine kinase is a therapeutic target in pre-B cell acute lymphoblastic leukemia. *Blood* **2013**, *122*, 1599–1609.
- (6) Linger, R. M.; Cohen, R. A.; Cummings, C. T.; Sather, S.; Migdall-Wilson, J.; Middleton, D. H.; Lu, X.; Baron, A. E.; Franklin, W. A.; Merrick, D. T.; Jedlicka, P.; Deryckere, D.; Heasley, L. E.; Graham, D. K. Mer or Axl receptor tyrosine kinase inhibition promotes apoptosis, blocks growth and enhances chemosensitivity of human non-small cell lung cancer. *Oncogene* **2013**, *32*, 3420–3431.

(7) Liu, J.; Zhang, W.; Stashko, M. A.; DeRyckere, D.; Cummings, C. T.; Hunter, D.; Yang, C.; Jayakody, C. N.; Cheng, N.; Simpson, C.; Norris-Drouin, J.; Sather, S.; Kireev, D.; Janzen, W. P.; Earp, H. S.; Graham, D. K.; Frye, S. V.; Wang, X. UNC1062, a new and potent Mer inhibitor. *Eur. J. Med. Chem.* **2013**, *65*, 83–93.

(8) Schlegel, J.; Sambade, M. J.; Sather, S.; Moschos, S. J.; Tan, A. C.; Wings, A.; Deryckere, D.; Carson, C. C.; Trembath, D. G.; Tentler, J. J.; Eckhardt, S. G.; Kuan, P. F.; Hamilton, R. L.; Duncan, L. M.; Miller, C. R.; Nikolaishvili-Feinberg, N.; Midkiff, B. R.; Liu, J.; Zhang, W.; Yang, C.; Wang, X.; Frye, S. V.; Earp, H. S.; Shields, J. M.; Graham, D. K. MERTK receptor tyrosine kinase is a therapeutic target in melanoma. *J. Clin. Invest.* **2013**, *123* (5), 2257–2267.

(9) (a) Liu, J.; Yang, C.; Simpson, C.; DeRyckere, D.; Van, D. A.; Miley, M. J.; Kireev, D.; Norris-Drouin, J.; Sather, S.; Hunter, D.; Korboukh, V. K.; Patel, H. S.; Janzen, W. P.; Machius, M.; Johnson, G. L.; Earp, H. S.; Graham, D. K.; Frye, S. V.; Wang, X. Discovery of small molecule mer kinase inhibitors for the treatment of pediatric acute lymphoblastic leukemia. *ACS Med. Chem. Lett.* **2012**, *3*, 129–134. (b) Wang, X.; Liu, J.; Yang, C.; Zhang, W.; Frye, S.; Kireev, D. Preparation of Pyrazolopyrimidine Compounds for the Treatment of Cancer. WO2011146313A1, 2011.

(10) (a) Mathieu, S.; Gradl, S. N.; Ren, L.; Wen, Z.; Aliagas, I.; Gunzner-Toste, J.; Lee, W.; Pulk, R.; Zhao, G.; Alicke, B.; Boggs, J. W.; Buckmelter, A. J.; Choo, E. F.; Dinkel, V.; Gloor, S. L.; Gould, S. E.; Hansen, J. D.; Hastings, G.; Hatzivassiliou, G.; Laird, E. R.; Moreno, D.; Ran, Y.; Voegtli, W. C.; Wenglowksy, S.; Grina, J.; Rudolph, J. Potent and selective aminopyrimidine-based B-Raf inhibitors with favorable physicochemical and pharmacokinetic properties. *J. Med. Chem.* **2012**, *55* (6), 2869–2881. (b) Zhang, G.; Ren, P.; Gray, N. S.; Sim, T.; Liu, Y.; Wang, X.; Che, J.; Tian, S.-S.; Sandberg, M. L.; Spalding, T. A.; Romeo, R.; Iskandar, M.; Chow, D.; Martin Seidel, H.; Karanewsky, D. S.; He, Y. Discovery of pyrimidine benzimidazoles as Lck inhibitors: part I. *Bioorg. Med. Chem. Lett.* **2008**, *18* (20), 5618–5621. (c) Furet, P.; Caravatti, G.; Guagnano, V.; Lang, M.; Meyer, T.; Schoepfer, J. Entry into a new class of protein kinase inhibitors by pseudo ring design. *Bioorg. Med. Chem. Lett.* **2008**, *18* (3), 897–900.

(11) Chen, K.; Peterson, R.; Math, S. K.; LaMunyon, J. B.; Testa, C. A.; Cefalo, D. R. Lithium trihydroxy/triisopropoxy-2-pyridylborate salts (LTBS): synthesis, isolation, and use in modified Suzuki–Miyaura cross-coupling reactions. *Tetrahedron Lett.* **2012**, *53* (36), 4873–4876.

(12) Wang, L.; Cui, X.; Li, J.; Wu, Y.; Zhu, Z.; Wu, Y. Synthesis of biaryls through a one-pot tandem borylation/Suzuki–Miyaura cross-coupling reaction catalyzed by a palladacycle. *Eur. J. Org. Chem.* **2012**, 595–603.

(13) (a) Pommereau, A.; Pap, E.; Kannt, A. Two simple and generic antibody-independent kinase assays: comparison of a bioluminescent and a microfluidic assay format. *J. Biomol. Screening* **2004**, *9* (5), 409–416. (b) Dunne, J.; Reardon, H.; Trinh, V.; Li, E.; Farinas, J. Comparison of on-chip and off-chip microfluidic kinase assay formats. *Assay Drug Dev. Technol.* **2004**, *2* (2), 121–129. (c) Bernasconi, P.; Chen, M.; Galasinski, S.; Popa-Burke, I.; Bobasheva, A.; Coudurier, L.; Birkos, S.; Hallam, R.; Janzen, W. P. A chemogenomic analysis of the human proteome: application to enzyme families. *J. Biomol. Screening* **2007**, *12* (7), 972–982.